LASER & PHOTONICS REVIEWS

Laser Photonics Rev. **5**, No. 2, 308–321 (2011) / **DOI** 10.1002/lpor.201000014

Abstract Topology optimization is a computational tool that can be used for the systematic design of photonic crystals, waveguides, resonators, filters and plasmonics. The method was originally developed for mechanical design problems but has within the last six years been applied to a range of photonics applications. Topology optimization may be based on finite element and finite difference type modeling methods in both frequency and time domain. The basic idea is that the material density of each element or grid point is a design variable, hence the geometry is parameterized in a pixel-like fashion. The optimization problem is efficiently solved using mathematical programming-based optimization methods and analytical gradient calculations. The paper reviews the basic procedures behind topology optimization, a large number of applications ranging from photonic crystal design to surface plasmonic devices, and lists some of the future challenges in non-linear applications.

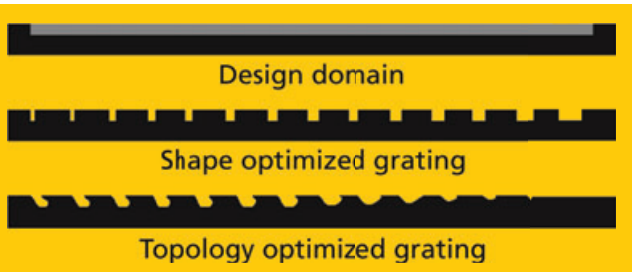

Topology optimization for nano-photonics

Jakob S. Jensen * **and Ole Sigmund**

1. Introduction

Nano-photonics comprises photonic crystal based waveguides and structures [1–3], surface plasmonic structures [4], perfect imaging by meta materials [5], extraordinary transmission [6] and many other nano-structured optical devices. Common for all is that smart spatial placement or distribution of dielectric materials, air and/or metals determines their functionality. For example the periodic modulation of dieletric/void materials creates photonic band gap materials which in turn may be disturbed by rows of defects creating photonic crystal based waveguides. Likewise, carefully shaped and distributed U-shaped metallic conductors may create negative index materials for use in imaging and cloaking [7, 8]. Originally, all these applications were conceived by clever physicists with greatly developed intuition and physical insight. In the wake of these discoveries it is obvious to pose the inverse problems: what is the distribution of material that maximizes the transmission? – lowers the group velocity? – minimizes the metamaterial loss? etc.

Inverse problems may be solved with more or less design freedom and in more or less systematic ways. A simple question to ask is: what is the periodic placement and radius of circular holes that maximizes the photonic band gap? Such problems can be solved by producing gap maps for various hole arrangements and selecting the material with the largest band gap [9]. Likewise, one may ask the question: out of a periodic arrangement of rods, which should be kept and which should be removed in order to optimize wave-focussing? Such problems may be solved by Genetic Algorithms [10] and other evolutionary techniques [11] or more systematic and efficient gradient based methods. Common for these two specific examples and by far largest part of literature on inverse problems in nano-photonics is that holes are limited to be circular and regularly placed. However, nothing says that a circular hole is optimal – in fact the hole shape that maximizes the photonic band gap for planar periodic structures is hexagonal and not circular [12]. Of course manufacturing abilities may put limitations on the achievable minimum feature sizes but apart from this, it is clear that deferring from fixed circular holes and other simple geometrical features may dramatically increase the performance of nano-photonic devices.

An inverse method which can produce optimized geometries for nano-photonic devices without any constraint on geometrical shapes is the topology optimization method. The concept was originally developed for mechanical problems [13, 14] and is now an extremely important industrial tool for the weight optimal design of machine parts, cars, airplanes and aerospace structures. The basic idea of the computational topology optimization approach is to define the design by a pixel representation, i. e. one design variable pr. finite element or finite difference node which can vary between 0 (void) or 1 (solid dielectric material). The optimized structure is then described by a bitmap (or voxel) picture c. f. Fig. 1. The iterative topology optimization approach is based on repeated finite element (or finite difference) analyses, gradient computations and updates by deterministic mathematical programming-based optimization procedures. Usually, convergence is obtained within a couple of hundred iterations each comprising one system analysis and a gradient computation which turns out to be very cheap. The concept of topology optimization has previously been applied to a number of alternative applications, including negative Poisson's ratio [15], negative thermal expansion [16], MEMS [17], micro fluidics [18], phononic band and structure design [19] as well as antenna design [20, 21], and is continuously being adapted to new

Department of Mechanical Engineering, Technical University of Denmark, Nils Koppels Alle, B. 404, Kgs. Lyngby 2800, Denmark
* Corresponding author: e-mail: jsj@mek.dtu.dk

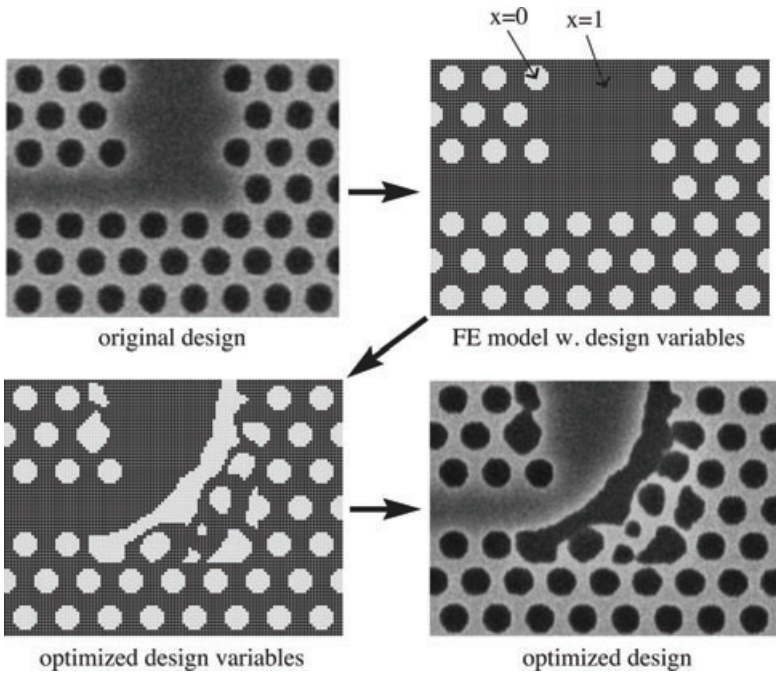

Figure 1 Parametrization of the topology design problem.

application areas. A review on inverse material distribution methods applied to photonic crystals was given by Burger *et .al* [22] but to the authors' best knowledge the present review is the first on the broader topic of nano-photonics design by topology optimization.

The review is organized as follows. In Sect. 2 we introduce the basic Partial Differential Equations (PDEs) and boundary conditions (BCs) and their discretization using Finite Element notation. Then we discuss the topology optimization design parametrization, the associated sensitivity analysis, the formulation of the optimization problem and finally a discussion on mesh-control and mathematical well-posedness. Sect. 3 discusses a wide range of applications – from photonic crystals over non-linear systems to plasmonics. In Sect. 4 we conclude the overview and give some guidelines to future research.

2. Topology optimization

In the following sections we describe the basics of the topology optimization procedure. This comprises the numerical modeling, design parametrization, sensitivity analysis and an overview of different optimization and regularization schemes.

2.1. Numerical modeling in frequency and time domain

The basis for the optimization scheme is a forward analysis of the relevant field problem. This analysis may be carried out in a time domain using a numerical integration algorithm. Alternatively, we may perform the analysis in the frequency domain in order to find the steady-state behavior for time-harmonic excitation of a device or to find eigensolutions to a photonic crystal unit cell problem or a waveguide supercell problem.

For the photonic devices considered, the behavior is governed by the PDEs (source free Maxwell equations):

$$\nabla \times \mathbf{H} = \varepsilon_0 \varepsilon_r \frac{\partial \mathbf{E}}{\partial t}, \tag{1}$$

$$\nabla \times \mathbf{E} = -\mu_0 \frac{\partial \mathbf{H}}{\partial t} \tag{2}$$

in which $\mathbf{E} = (E_x\ E_y\ E_z)^T$ and $\mathbf{H} = (H_x\ H_y\ H_z)^T$ is the electric and magnetic vector field, respectively. The free-space permittivity and permeability are ε_0 and μ_0 and the relative permittivity is symbolized by ε_r.

Many relevant design problems for photonic devices, such as photonic crystal waveguides, photonic crystal fibers, etc. can be performed on the basis of a relevant 2D simplification of the full 3D equations. For TM-polarized waves we have that $\mathbf{E} = (0\ 0\ E_z)^T$ and $\mathbf{H} = (H_x\ H_y\ 0)^T$. Inserting this into Eqs. (1)–(2) yields an equation that governs the out-of-plane component of the electric field E_z:

$$\nabla^2 E_z - \frac{\varepsilon_r}{c^2} \frac{\partial^2 E_z}{\partial t^2} = 0 \tag{3}$$

in which $c = \frac{1}{\sqrt{\mu_0 \varepsilon_0}}$ is the free-space speed of light.

For TE-polarized waves, $\mathbf{E} = (E_x\ E_y\ 0)^T$ and $\mathbf{H} = (0\ 0\ H_z)^T$. This leads to an equation for the out-of-plane component of the magnetic field H_z:

$$\nabla \cdot \left(\frac{1}{\varepsilon_r} \nabla H_z \right) - \frac{1}{c^2} \frac{\partial^2 H_z}{\partial t^2} = 0 \tag{4}$$

For topology optimization problems based on transient response, numerical simulations can be based on a spatially

discretized version (e. g. a FE model) of either of the above mentioned equations. In many cases a 2D computational model will suffice leading to substantial computational savings, but this will depend on the specific application and/or operating conditions. Often the optimization problem can with advantage be formulated in the frequency domain on the basis of the steady-state response to time-harmonic excitation. The steady-state behavior can be expressed in terms of the frequency as:

$$E_z(\mathbf{x},t) = E_z(\mathbf{x})e^{i\omega t}, \tag{5}$$

$$H_z(\mathbf{x},t) = H_z(\mathbf{x})e^{i\omega t} \tag{6}$$

and with this assumption inserted into the 2D Eqs. (3)–(4), the TM- and TE-polarized equations take the generalized appearance:

$$\nabla\cdot(A\nabla u) + B\omega^2 u = 0 \tag{7}$$

in which $A = 1$, $B = \varepsilon_r c^{-2}$ and $u = E_z$ for TM-polarized waves and $A = 1/\varepsilon_r$, $B = c^{-2}$ and $u = H_z$ for the TE-polarized case.

Most of the examples presented later will be based on a FE model of Eq. (7) which is a standard scalar Helmholtz equation. As a note it should be emphasized that the same equation can also be used to model certain types of elastic wave propagation [19] as well as acoustic wave propagation [23] with the proper choice of the coefficients A and B.

2.1.1. Boundary conditions

The presented PDEs must be combined with a set of boundary conditions (and for transient problems additionally a set of initial conditions) in order to pose the complete problem. With the proper choice of boundary conditions we are able to specify wave excitation and/or sections of the boundary through which waves are allowed to be transmitted without reflections.

For the case of steady-state analysis with Eq. (7), a general Robin boundary condition:

$$\mathbf{n}\cdot(A\nabla u) + i\omega\sqrt{AB}u = 2i\omega\sqrt{AB}u_0 \tag{8}$$

can be used on specific boundary sections to ensure absorption of waves of frequency ω and wave speed $\sqrt{A/B}$ and the emission of waves with amplitude u_0 propagating away from the boundary.

The Robin boundary condition causes reflections when the wave incidence angle to the boundary is not normal. Also if the propagation characteristics are different than specified in the BC (frequency and wave speed) reflections will occur. The latter situation is especially relevant for simulation of photonic crystal waveguides, for which the propagation characteristic is an intrinsic property of the structure and not necessarily known a priori. In order to obtain a low reflection of waves for a wide range of incidence angles and for various propagation characteristics, Perfectly Matched Layers (PMLs) [24] are often applied. These layers constitute extra absorbing domains surrounding the usual computational domain. Inside the PMLs the field satisfies the following PDE:

$$\frac{\partial}{\partial x}\left(\frac{s_y}{s_x}A\frac{\partial u}{\partial x}\right) + \frac{\partial}{\partial y}\left(\frac{s_x}{s_y}A\frac{\partial u}{\partial y}\right) + \omega^2 s_x s_y B u = 0 \tag{9}$$

in which s_x and s_y are complex damping functions that ensure the dissipation of the waves within the layers. These functions can be chosen differently, but a popular form is [25]:

$$s_x = 1 - i\sigma\Delta x^2, \tag{10}$$

$$s_y = 1 - i\sigma\Delta y^2 \tag{11}$$

in which Δx and Δy are the perpendicular distances from a point in the PML layer to the boundary of the real computational domain. The parameter σ denotes the strength of the damping. It should be noted that if σ is chosen too large, reflections will occur at the boundary between the real and the PML domain, due to the spatial discretization of the problem. On the other hand, if σ is chosen too small and the dimensions of the PML layer are insufficient, reflections will occur at the outer boundary of the PML domain. It is noted that on the boundary between the computational domain and the PML, $s_x = s_y = 1$ and Eq. (9) reduces to Eq. (7). This is also the case if $\sigma = 0$. The use of PMLs in conjunction with topology optimization is especially recommendable since the material distribution is not known a priori, and consequently the angle of incidence and the propagation characteristics are not known. The use of PMLs is however expensive in terms of computational efforts.

For transient problems the formulation and implementation of PML layers is more cumbersome. A recent implementation for a topology optimization problem of a 2D photonic structure can be found in [26].

Alternatively, one may enforce propagating solutions by considering only a section, a unit cell or a super cell (comprising several unit cells) and then enforcing the Bloch-wave condition [27]:

$$u(\mathbf{r}+\mathbf{R}) = u(\mathbf{r})e^{i\mathbf{kr}} \tag{12}$$

in which $\mathbf{k}$ is the wavenumber and $\mathbf{R}$ the lattice vector. This approach can be used to identify propagating modes in a structure composed of identical unit cells (a periodic structure of photonic crystal) or in periodic waveguides represented by supercells.

2.1.2. Finite element model

The topology optimization method lends itself to a finite element model of the governing PDE. However, it should be emphasized that any discretization method based on local approximations, such a finite differences or finite volumes, readily fits into the optimization framework.

Regardless of the choice of discretization, we consider a model of the following form:

$$\mathbf{M}\ddot{\mathbf{u}} + \mathbf{C}\dot{\mathbf{u}} + \mathbf{K}\mathbf{u} = \mathbf{f}(t) \tag{13}$$

in which **u** is a vector containing the unknown discretized element, nodal or cell values of the field u. The matrices **M**, **C** and **K** are formed as part of the discretization procedure, and depend on the local values of the material properties A and B (see e. g. standard Finite Element literature or more specifically [28]).

The excitation term on the rhs. of Eq. (12) originates in the inhomogeneous boundary condition terms (such as the rhs. of Eq. (8)). The absorbing part of the same boundary condition will enter into the matrix **C**. The use of PMLs or Bloch-wave BCs (12) results in complex entries in the matrices **M** and/or **K**.

In the frequency domain the steady-state response is found under the assumption that the excitation is time-harmonic:

$$\mathbf{f}(t) = \mathbf{f}e^{i\omega t} \tag{14}$$

and combined with a time-harmonic assumption on the solution:

$$\mathbf{u}(t) = \mathbf{u}e^{i\omega t} \tag{15}$$

this leads to the following set of linear equations:

$$\mathbf{S}\mathbf{u} = \mathbf{f} \tag{16}$$

in which the system matrix **S** is given as

$$\mathbf{S} = -\omega^2\mathbf{M} + i\omega\mathbf{C} + \mathbf{K} \tag{17}$$

The frequency domain formulation yields a response for a specific frequency ω. If we seek the response for multiple frequencies (e. g. for a broadband wave signal) the solution procedure presented above becomes very expensive since Eq. (16) needs to be solved for each frequency. In [28] it was suggested to use Pade approximants to efficiently compute the response in a frequency band as a basis for multiple frequency optimization problems.

If we wish to produce band diagrams and/or identify propagating modes for a periodic structure an eigenvalue problem must be solved. This is obtained with vanishing wave excitation ($\mathbf{f} = \mathbf{0}$) and damping matrix ($\mathbf{C} = \mathbf{0}$). We then obtain the following eigenvalue problem:

$$\left(-\omega^2\mathbf{M}(\mathbf{k}) + \mathbf{K}(\mathbf{k})\right)\mathbf{u} = \mathbf{0} \tag{18}$$

in which the explicit dependence of the wavevector **k** indicates that Bloch-wave boundary conditions have been enforced. The eigenvalue problem yields, for each **k**, a set of eigensolutions $(\omega_i, \mathbf{u}_i)$.

2.1.3. Solution procedures

The eigenvalue problem stated in Eq. (18) can be solved by efficient algorithms [27] and for the steady-state problem in Eqs. (16)–(17) a wide variety of efficient direct or iterative solvers are available. It should be noted, however, that the linear system is complex and not positive definite which puts restrictions on the class of iterative solvers that can be applied.

For the full transient problem in Eq. (10), the state equation together with appropriate initial conditions, can be simulated either with the use of implicit or explicit time integration schemes. From an optimization point of view it is not essential which type of solver is chosen but it should be noted that explicit solvers are usually faster, especially in conjunction with a lumped **M**-matrix which allows for a cheap inversion in the solution procedure.

2.2. Design parametrization

The basic feature of the topology optimization method is the, in principle, unlimited design freedom facilitated by the formulation as a material distribution method. This implies that the design is parameterized locally so that the material properties at each spatial point in the structure is a design variable to be optimized.

With a finite element model, a standard procedure, known as the density approach [29], is to introduce an element design variable that controls the material properties of that specific element. A discrete element design variable, χ_e, can be introduced so that:

$$\chi_e = \begin{cases} 0, & \text{if material 1 in element} \\ 1, & \text{if material 2 in element} \end{cases} \tag{19}$$

Hence, the optimization problem will be to find the optimal distribution of the two materials in the domain of interest.

However, since we aim at using a gradient based optimization algorithms, we convert the discrete element variables into continuous ones:

$$0 \leq \rho_e \leq 1 \tag{20}$$

and combine these variables with a material interpolation law that provides the material properties of the specific elements [30]. Examples of simple linear material interpolation laws that has been applied successfully to nano-photonic device design are:

$$A_e = A_1 + \rho_e(A_2 - A_1), \tag{21}$$

$$B_e = B_1 + \rho_e(B_2 - B_1) \tag{22}$$

in which the values A_1, A_2, B_1, B_2 are the specific values of the material properties (e. g. the permittivity) of the two available materials (e. g. dielectric and void).

In the case of TE-polarized waves, the material interpolation specified in Eq. (21) gives the following interpolation of the element permittivity: $\frac{1}{\varepsilon_r} = \frac{1}{\varepsilon_{r1}} + \rho_e(\frac{1}{\varepsilon_{r2}} - \frac{1}{\varepsilon_{r1}})$. This interpolation has been shown to work nicely for many problems. However, positive experience with an alternative parametrization that reads $\varepsilon_r = \varepsilon_{r1} + \rho_e(\varepsilon_{r2} - \varepsilon_{r1})$ has also been reported [31].

The use of a continuous design variable in the element provides the essential advantage that we are able to use gradient-based optimization algorithms that efficiently can provide us with a good optimized solution for thousands or

perhaps millions of design variables. In the discrete case we would be forced to keep the number of design variables at a much more moderate level. However, a drawback is that the introduction of continuous variables creates the possibility that "intermediate" or "grey" variables appear in the optimized designs. The material properties of the corresponding grey elements do not correspond to any of the two available materials and they must be eliminated before an optimized device can be presented. Several penalization techniques have been developed to remedy this problem, with some of them utilizing material interpolation schemes that "favorize" design variables with values 0 or 1. A popular scheme for mechanics applications is the SIMP-scheme [29] where intermediate densities are made unfavourable. However, in optimization problems where a large local reflection of waves is required, well defined structures seem to appear automatically and there is no need for penalization of intermediate design variables. This happens since intermediate design variables reduce the contrast between the materials and thus lead to a reduced reflection. It has later been shown for a general class of wave propagation problems that classical solutions (pure 0–1 designs) are optimal under certain conditions [32].

However, when the optimization problem is not strictly of the reflection type, the problem with intermediate densities may appear also for the design of nano-photonic devices. In this case, as an alternative to the SIMP-approach, a technique based on artificial damping in grey elements ("Pamping") has been successfully applied [28].

2.3. Sensitivity analysis

One of the great advantages of the topology optimization method is the complete design freedom facilitated by a large number of local design variables. However, only in conjunction with an efficient approach to computing design sensitivities, does this result in a feasible algorithm. As outlined in the following, the adjoint sensitivity calculation approach is a perfect match to a topology optimization scheme, since it provides sensitivity information at low computational cost, also with a large number of design variables.

However, in the case of bandgap and guided mode optimization problems we need only to compute the sensitivities of the eigenvalues. This can be done in a straightforward manner as:

$$\frac{\mathrm{d}\omega_i^2}{\mathrm{d}\rho_e} = \mathbf{u}_i^T \frac{d(\mathbf{K}-\omega_i^2\mathbf{M})}{d\rho_e}\mathbf{u}_i \tag{23}$$

in which it is assumed that the eigenvectors $\mathbf{u}_i$ have been normalized so that $\mathbf{u}_i^T\mathbf{M}\mathbf{u}_i = 1$. An additional complication arises if multiple eigenvalues appear which often happens in an optimization problem. In this case the sensitivity calculation must be modified [33, 34].

For the case of steady-state or transient response the adjoint approach is used to compute the sensitivities. We assume that the structure or device can be characterized by a performance measure (or objective function) written as:

$$\Phi_{\mathrm{FD}}(\mathbf{u},\rho) \quad \text{or} \quad \Phi_{\mathrm{TD}} = \int_0^{\mathscr{T}} c(\mathbf{u},\rho)dt \tag{24}$$

in which the subscripts FD and TD denote frequency and time domain, respectively. Here, $\mathscr{T}$ is the total simulation time for the transient computation.

The sensitivity of the objective function wrt. changes in a design variable is found by the chain rule:

$$\frac{\mathrm{d}\Phi}{\mathrm{d}\rho_e} = \frac{\partial\Phi}{\partial\rho_e} + \frac{\partial\Phi}{\partial\mathbf{u}}\frac{\partial\mathbf{u}}{\partial\rho_e} \tag{25}$$

The implicit derivative $\frac{\partial\mathbf{u}}{\partial\rho_e}$ cannot be computed in a straightforward manner. It can instead be eliminated by using the adjoint approach [35]. In the frequency domain this results in an adjoint equation:

$$\mathbf{S}^T\lambda = -\frac{\partial\Phi_{\mathrm{FD}}}{\partial\mathbf{u}} \tag{26}$$

and the corresponding sensitivity can be computed as:

$$\frac{\mathrm{d}\Phi_{\mathrm{FD}}}{\mathrm{d}\rho_e} = \frac{\partial\Phi_{\mathrm{FD}}}{\partial\rho_e} + 2\Re\left(\lambda^T\frac{\partial\mathbf{S}}{\partial\rho_e}\mathbf{u}\right) \tag{27}$$

It is here important to emphasize that the adjoint Eq. (26) should be solved only once, regardless of the number of design variables. Furthermore, if Eq. (16) is solved using a factorization method, and $\mathbf{S}$ is symmetric ($\mathbf{S}^T = \mathbf{S}$), the solution to Eq. (26) is simply obtained as an extra forward-backward substitution. This is computationally very cheap.

For the case of a transient problem the adjoint equation becomes:

$$\mathbf{M}^T\ddot{\lambda} + \mathbf{C}^T\dot{\lambda} + \mathbf{K}^T\lambda = -\left.\frac{\partial c}{\partial\mathbf{u}}\right|_{\mathscr{T}-t} \tag{28}$$

in which the rhs. should be evaluated at the "adjoint time" $\mathscr{T}-t$ as indicated. The transient equation can be solved using the same numerical procedure as the forward equation and should be combined with the following set of initial conditions:

$$\lambda(\mathscr{T}) = \dot{\lambda}(\mathscr{T}) = \mathbf{0} \tag{29}$$

When the adjoint variables have been computed the corresponding sensitivity becomes:

$$\frac{\mathrm{d}\Phi_{\mathrm{TD}}}{\mathrm{d}\rho_e} = \int_0^{\mathscr{T}}\left(\frac{\partial c}{\partial\rho_e} + \lambda^T\left(\frac{\partial\mathbf{M}}{\partial\rho_e}\ddot{\mathbf{u}} + \frac{\partial\mathbf{C}}{\partial\rho_e}\dot{\mathbf{u}} + \frac{\partial\mathbf{K}}{\partial\rho_e}\mathbf{u}\right)\right) \tag{30}$$

Again, the computation of the sensitivities, for an arbitrary number of design variables, constitutes only a simulation of one extra transient problem in addition to the numerical integration in Eq. (30). Thus, the adjoint approach is feasible also for very large problems. However, here it should be noted that a main challenge becomes the storage of the vector $\mathbf{u}$ for all time steps. The storage is necessary in order to compute the adjoint load (the rhs.) of Eq. (28) and the integral in Eq. (30). Workarounds have been suggested in which the entire time history for $\mathbf{u}$ is not stored but recomputed when needed.

It should be added that if the optimization problem is subject to various *constraints* then the sensitivities of these should be computed as well. Depending on analysis type the added computational cost per constraint may range from a few percent (extra right hand side in already factorized system) to almost 100% (transient problem).

2.4. Optimization schemes

The final form of the optimization problem may be

$$\left.\begin{aligned} &\min_{\rho} : \Phi(\rho) \\ &s.t. : g_0(\rho) = V(\rho)/V^* - 1 \leq 0 \\ &\quad : g_i(\rho) =\leq 0,\ i = 1,\ldots m \\ &\quad : 0 \leq \rho \leq 1 \end{aligned}\right\}, \tag{31}$$

where $V(\rho)$ is the volume of dielectric material, V^* is the upper bound on material usage and $g_i(\rho)$ are m additional design dependent constraints. This optimization problem may be solved very efficiently using mathematical programming techniques like the Method of Moving Asymptotes [36] assuming that the sensitivities have been computed using the adjoint method as outlined in Sect. 2.3. Alternative solvers are Sequential Quadratic or Linear Programming methods (SLP or SQP). The optimization problem may be reformulated for certain problems. For example the goal of maximizing the minimum transmission over a number of frequencies (i. e. ensuring wide band transmission) may be formulated as a max-min problem which is usually non-differentiable. However, the non-differentiability may be overcome by recasting the problem in a so-called bound formulation

$$\left.\begin{aligned} &\max : \beta \\ &s.t. : -g_i(\rho) + \beta \leq 0,\ i = 1,\ldots n \\ &\quad : g_{n+1}(\rho) = V(\rho)/V^* - 1 \leq 0 \\ &\quad : g_i(\rho) =\leq 0,\ i = (n+2),\ldots (n+m+2) \\ &\quad : 0 \leq \rho \leq 1 \end{aligned}\right\}, \tag{32}$$

where the first n constraint functions of $g_i(\rho)$ correspond to the transmission values for n frequencies. This concept can be further explored using Pade approximants c. f. [28].

2.5. Ill-posedness and manufacturability issues

As formulated above the optimization problems (31) and (32) are ill-posed and may result in designs that are difficult to manufacture. The ill-posedness is seen in designs that are not convergent with mesh-refinement and designs that have very small details like one element holes or material islands that are neither manufacturable nor make physical or mathematical sense. To avoid this, different regularization techniques may be added to the problem formulation. In image analysis and general inverse problems so-called Tikhonov regularizations are popular. However, these are usually implemented as penalization terms added to the objective functions and such terms may require careful tuning - especially when combined with problems that have many other constraints like the max-min formulation (32). Instead, the topology optimization community prefers image processing inspired filter regularization techniques. These techniques are extensively reviewed in [37, 38] but the most popular schemes are briefly introduced in the following.

A length scale may be introduced into the optimization problem by introducing image processing based filtering techniques into the optimization model. Viewing the design domain as an image consisting of pixels (voxels in 3d), a filter window of radius R may be introduced. Using this filter we may define a neighborhood N_e of each element e as the elements that lie within the filter radius

$$N_e = \{i \mid ||\mathbf{x}_i - \mathbf{x}_e|| \leq R\}. \tag{33}$$

The regularization may now be implemented as a heuristic filtering of the element sensitivities [39]

$$\widetilde{\frac{\partial f}{\partial \rho_e}} = \frac{\sum_{i \in N_e} w(\mathbf{x}_i)\rho_i \frac{\partial f}{\partial \rho_i}}{\rho_e \sum_{i \in N_e} w(\mathbf{x}_i)}, \tag{34}$$

where v_i denotes the volume of element i and the weighting function $w(\mathbf{x}_i)$ is given by the linearly decaying (cone-shape) function

$$w(\mathbf{x}_i) = R - ||\mathbf{x}_i - \mathbf{x}_e||. \tag{35}$$

Alternatively one may implement a theoretically more well-founded density filtering scheme where element densities are modified according to

$$\tilde{\rho}_e = \frac{\sum_{i \in N_e} w(\mathbf{x}_i) v_i \rho_i}{\sum_{i \in N_e} w(\mathbf{x}_i) v_i}, \tag{36}$$

as suggested in [40, 41].

Both schemes introduce a length-scale of R into the design problem, i. e. no features like holes or solid bridges will be smaller than R. However, this feature size control comes at the cost of the introduction of a grey-scale transition region where design variables take non 0/1 values in a rim of width R around the boundaries. To avoid this one may gradually decrease the filter size during the design process in a continuation approach but with the risk of introducing new small features. Alternatively, recently proposed projection schemes [38, 42, 43] building on (36) introduce ways to ensure both the length scale R and black and white solutions. Even more recently, these projection schemes have been combined to robust formulations that ensure insensitivity to under- or overetching during the design process [44–46].

Most of the previously presented results on nano-photonics and topology optimization by the authors' research group have been based on the sensitivity filter (34 combined with a continuation approach. However, it is expected that the projection approaches will take over in the future since they ensure better and crisper length-scale control and allow for robust design formulations. Some examples can be seen in [26, 47, 48].

In addition it should be mentioned that for the dynamic optimization problems we usually encounter multiple local optima. This poses a great challenge for any optimization method including gradient-based topology optimization.

One approach that has been used with success is to impose a regularization of the problem by adding large amounts of artificial damping in the initial phase of the optimization iterations [28]. This was demonstrated to smooth out the response function and eliminate local optima associated with resonance phenomena.

3. Applications

In the following we will review the recent years applications of the topology optimization to eigenvalue, steady-state and transient problems in nano-photonics.

3.1. Photonic crystals

Many nano-photonic devices are based on two-dimensional photonic crystals. The periodic arrangement of dielectric pillars in air, or air holes in a dielectric creates a photonic bandgap that can be used to confine light and to create unique dispersion properties.

The basic optimization problem that can be formulated for a photonic crystal is to find the material layout that maximizes the photonic bandgap. The problem was studied first in [49, 50] who found optimal distributions of dielectric material and air. This was done by considering a single unit cell, and in their work they considered both TE- and TM-polarization for square and hexagonal unit cells.

One way to formulate the bandgap optimization problem is to consider the relative bandgap size. This can be measured as the difference between the lowest point on band $j+1$ and the highest point on band j (illustrated in Fig 2top). The difference is normalized with the mean value:

$$\frac{\Delta\omega}{\omega_0} = \frac{\min\limits_{\mathbf{k}} \omega_{j+1} - \max\limits_{\mathbf{k}} \omega_j}{\frac{1}{2}\left(\min\limits_{\mathbf{k}} \omega_{j+1} + \max\limits_{\mathbf{k}} \omega_j\right)} \tag{37}$$

By using the formulation in Eq. (37) it is possible to maximize the gap between any two bands j and $j+1$ in the band spectrum.

In [12] this approach was used to systematically open up and maximize all band gaps for $j = 1$ to 15 for both TE- and TM-polarized waves. Surprisingly the study showed a simple geometric systematism for the optimal photonic crystal structures:

(Near)optimal band gap structures for gaps between bands n and $n+1$ can be obtained by a geometric rule. For the TM-polarization the optimal unit cell structure consists of n elliptic rods with centers defined by the generators of the optimal centroidal Voronoi tesselation and the optimal unit cells for the TE-polarization corresponds to the walls of above tesselation. The overall optimal band gap is obtained for $n = 1$ in both cases corresponding to a triangular pattern of circular rods in the TM-case and a triangular pattern of hexagonal (not circular) holes for the TE-case. Composite pictures showing topology optimized unit cell structures as well as optimal tesselations are shown for $j = 1$ and 3 are shown in Fig. 2.

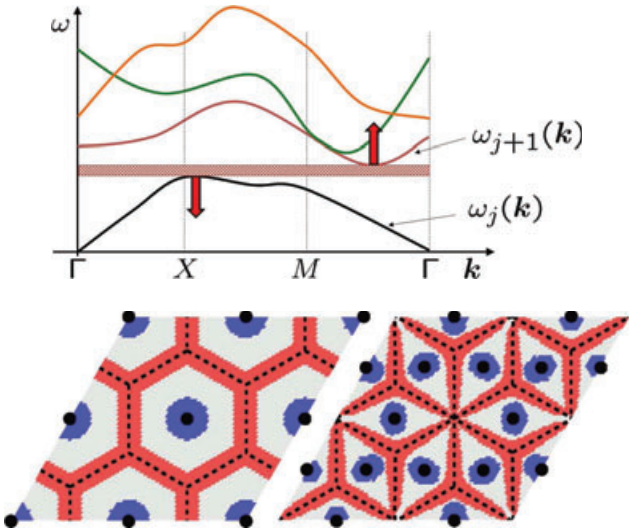

Figure 2 (online color at: www.lpr-journal.org) Top: Sketch of optimization goal for maximizing the band gap between bands j and $j+1$. Bottom: Composite pictures for topology optimized periodic structures (2 by 2 cells) obtained for $j = 1$ and $j = 3$. Colors indicate dielectric material (red for the TE polarized structures and blue for the TM case) and grey indicates void. Dashed lines indicate optimal centroidal Voronoi tesselations for 1 and 3 generating points (black dots). From [12].

These results were obtained for moderate dielectric contrast. In the low contrast case [51] reports larger bandgaps using another modeling procedure and quasi-periodic structures.

An interesting application of topology optimization to periodic structures which has not attracted too much attention so far is the design of reflecting [52] and absorbing surfaces.

3.2. Slow Light

An important nano-photonics subject is the engineering of slow light waveguides or other specified dispersion relations. Slow light structures are used for delay lines in signal processing and may ensure better interaction with quantum dots for active devices. Concerning slow light, several works have considered the movement or scaling of holes close to the defect [53, 54] in order to obtain constant low group velocity.

Topology optimization of slow light devices is based on super cell modeling but may be attacked in different ways. In [47] the super cell was excited with harmonic waves with even or odd symmetries. The goal was to maximize intensity in the core for a number of prescribed wavenumber/frequency pairs (k_i^*, ω_i^*) for the even modes and to constrain the intensity for the odd modes. In this way the authors achieved the prescribed even mode dispersion curve and at the same time they avoided multimodality of the guided modes. The weakness of this approach is that the

prescribed dispersion relation only is weakly enforced in the design problem and hence it seems to be a better idea to work directly with the wave-number/eigenvalue pairs from a conventional Bloch-wave analysis of the unit cell. This idea is used in [45] where a bandgap is enforced by constraints like Eq. (37) and with the goal of minimizing the least square norm of the difference between prescribed (k_i^*, ω_i^*) pairs and actual $(k_i(\rho), \omega_i(\rho))$ pairs for the guided mode. This study includes the robust formulation discussed in Sect. 2.5 which leads to a clear and well-defined blue-print design but also ensures that structures which are slightly under- or over-etched also perform as desired. An example is shown in Fig. 3 where the middle structure is the blue-print design and the left and right structures are the over- and under-etched designs, respectively.

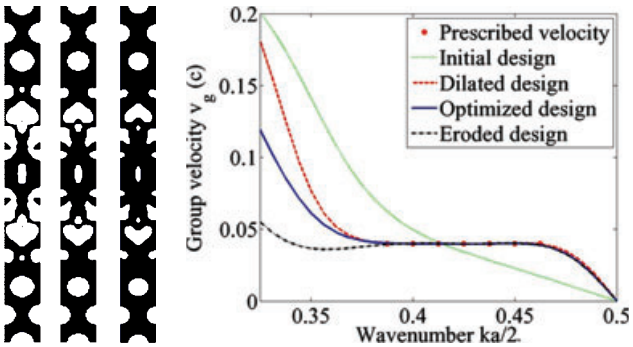

Figure 3 (online color at: www.lpr-journal.org) Topology optimization of slow light crystal using a robust design formulation. Left: the over-etched, perfect (blue-print) and under-etched super cells and Right: Dispersion curves showing that all three structures have constant low group velocities in a wide wave-number range. From [45].

3.3. Waveguides

We have demonstrated that topology optimization of unit cells can lead to photonic crystals with enlarged bandgaps which may increase the operational range of a corresponding photonic device. Furthermore, optimization of a supercell can result in slow light waveguides or waveguides with designated dispersion properties.

However, nano-photonic waveguide based devices may still experience significant losses due to un-optimized bends and junctions. The problem of finding the optimal material distribution in waveguide bends using topology optimization was first addressed in [55]. Here, the waveguide was based on a 2D photonic crystal for with a square unit cell containing a circular inclusion of a dielectric material surrounded by air. A single line of dielectric inclusions was removed to create a waveguide that allows waves to propagate – a guide mode. It was observed that creating a 90-degree bend in the waveguide resulted in a significant transmission loss due to reflections at the discontinuity. The losses would significantly deteriorate any device comprising such a bend and several design modifications had previously been suggested

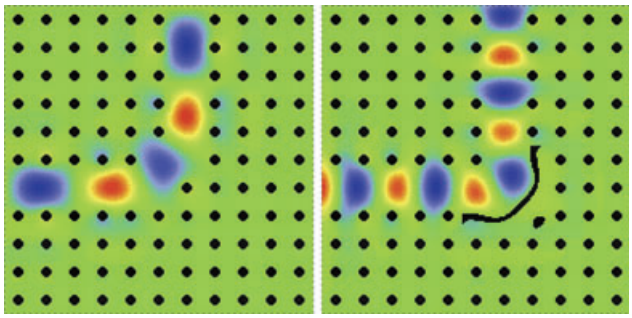

Figure 4 (online color at: www.lpr-journal.org) Left: previously best reported waveguide bend for low loss transmission of TM-polarized waves. Right: topology optimized bend structure showing a significantly lower loss for a large range of wave frequencies/wavelengths. From [55].

in order to maximize the power flow though the device. Fig. 4a shows an example of a structure suggested in [56] which has a very low loss in a narrow frequency band.

Fig. 4b shows the topology optimized material distribution. The design is obtained by maximizing the sum of the transmitted power for the three frequencies in the range of interest. The resulting structure has a non-intuitive appearance very different from structures reported in precedent studies and it outperforms them by having a very low loss of less than 0.3 % in a broad frequency range.

The performance measure used in this study is the power transmission. The instantaneous power flow can be computed as:

$$\mathbf{P} = \mathbf{E} \times \mathbf{H} \tag{38}$$

which in the case of planer polarized and time-harmonic waves reduces to the following equation for the time-averaged power flow:

$$\overline{\mathbf{P}_{\mathrm{TM}}} = \frac{1}{2\mu_0\omega}\Re\left(-iE_z\nabla E_z^*\right) \tag{39}$$

for the case of TM-polarization and

$$\overline{\mathbf{P}_{\mathrm{TE}}} = \frac{1}{2\varepsilon_0\varepsilon_r\omega}\Re(iH_z^*\nabla H_z) \tag{40}$$

for TE-polarization. For a specific waveguide either the x or the y component of the time averaged power flow is considered.

The 90-degree bend was later followed by topology optimization studies of similar waveguide configurations e. g. the optimization of a T-junction that transmits 50% of its energy in upwards and 50% downwards without reflections at the junction [28]. Also the waveguide termination was optimized in order to improve the directivity of the wave propagation from the output waveguide port [57]. However, these types of waveguides with dielectric rods in air, are rather complicated to fabricate and also prone to significant out-of-plane losses. Thus, so far, the performance of the optimized structures has not been validated by experimental results.

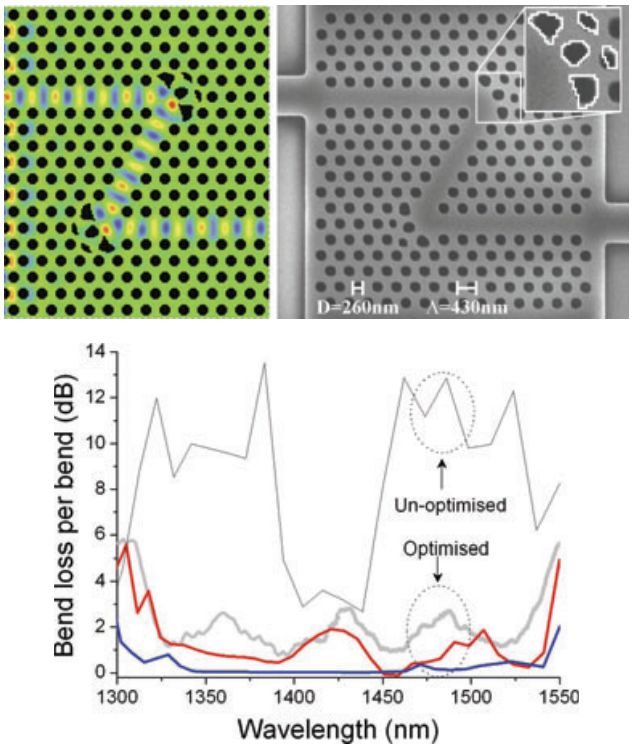

Figure 5 (online color at: www.lpr-journal.org) Top left: topology optimized Z-bend consisting of two 120-degree waveguide bends. Top right: fabricated structure indicating with white contour line the optimized hole geometries. Bottom: measured loss/bend of the fabricated optimized structure (thick grey), fabricated unoptimized (thin dashed). Shown also are numerically predicted losses which 2D finite element and 3D FDTD computations. From [58].

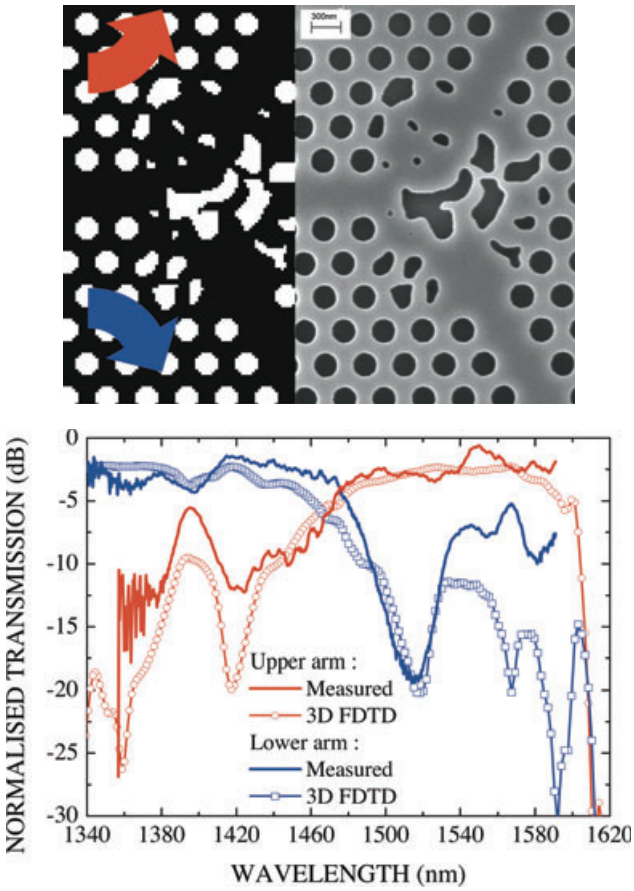

Figure 6 (online color at: www.lpr-journal.org) Waveguide splitter with advanced functionality. Short waves propagate though lower channel and longer waves though upper channel. Top: optimized and fabricated structures. Bottom: measured transmission for the fabricated structure. From [65].

On the other hand, photonic crystal structures made from air holes in a dielectric are much more amenable to fabrication and thus experimental validation. The first waveguide structure to be optimized using topology optimization for such a configuration was the "Z-bend" [58]. The Z-bend consists of two consecutive 120-degree bends in a waveguide created from a photonic crystal with a triangular configuration of air holes. The generic configuration, without any optimization, results in large reflection losses at the two waveguide bends, and consequently the transmitted power through the structure is very small. An attempt to increase the transmission was made in the computational study [59] in which the positions of a number of holes near the bends were perturbed. In [58] the first set of topology optimized 120-degree bends were demonstrated and are shown in Fig. 5. As it appears, holes in the outer region of the bend have been modified and have irregular shapes. The fabricated structure shows the intended hole geometries with white contour lines. Although the fabricated structure does not exactly match the intended, the performance was demonstrated to be very good and significantly better than the previous structures for a wide range of frequencies.

The successful optimization of the Z-bend waveguide, led to a large number of topology optimization studies of different kinds of bends and junctions in similar photonic crystal waveguide configurations. In [60] a 60-degree bend was optimized and a loss of less than 1dB over a 200nm wavelength range was reached and also a Y-splitter and a 90-degree bend were optimized [61, 62]. In [63] a waveguide intersection was optimized in order to provide for maximum transmission and minimum crosstalk. A waveguide taper structure was optimized in [64] providing a minimum of loss in the connection between a simple ridge waveguide and a photonic crystal waveguide.

These optimized photonic crystal building blocks may be useful in future integrated photonic circuits. But also components with more advanced functionality are relevant and Fig. 6a shows a topology optimized wavelength splitter. Here, the wave is split to have full transmission of shorter waves (below 1480 nm) through the lower output waveguide whereas longer waves (above 1480 nm) should propagate through the upper output waveguide. The optimized design is quite complicated with fine structural details in order to meet the objective[1]. Fig. 6b illustrates the corresponding

[1] The fabrication of this device was performed with nano-imprint lithography which nicely reproduces the small features in the design [65].

transmission plot where it is seen that the desired functionality is obtained with reasonable success and with a noticeable loss of around 2–3 dB occurs in both channels. This loss is caused by the difficulty of the optimization problem.

These examples of optimized component are all based on waveguides carved out in photonic crystal structures. This provides a convenient basis for confinement of the light useful for waveguiding purposes. However, another type of waveguides, usually known as strip or ridge waveguides, are applicable to photonic circuits as well. These are strips of dielectric material placed on a substrate and surrounded by air and may provide perfect waveguiding for straight guides. However, the problems at bends and junctions are even more severe than for photonic crystal waveguides in that the waves are no longer confined to the guide and additional in-plane scattering losses can occur. In [31, 66, 67] several different waveguiding structures were optimized and the cross-section of a ridge waveguide has also recently been topology optimized [68].

The waveguide examples shown here all required moderate computational effort and were created using a standard desktop computer. As a typical example the wavelength splitter was modeled using around 140000 quadratic elements with about 3000 design variables. A single analysis was performed in approximately 10 seconds, implying that a full optimization run for multiple frequencies could be run overnight.

3.4. Filters and pulse modulation

Design of filters and pulse modulation devices are also obvious applications for the topology optimization method. The two applications are closely related since both can be defined as inverse problems of tailoring the transmission function. However, whereas frequency filters may be designed efficiently both in frequency and time domain, it is more efficient and straightforward to design for pulse conversion in the time domain.

Starting with the frequency domain, minimization of the transmission for a given frequency results in crystal-like structures with large band gaps centered at the target frequency [19, 69]. Likewise one may design multi-channel stop band structures by minimizing transmission for two or more separated frequencies simultaneously. Alternatively, the problem may be defined in the time domain by minimizing the transmitted energy for one or more pulses with different carrier frequencies and bandwidths, resulting in corresponding transmission dips [70].

Pulse modulation problems like conversion of Gaussian to square or sawtooth pulses, generation of pulse trains, sharpening of pulses a. o. may in principle be designed in the frequency domain. The principle would be to minimize the mean square norm of the difference between the prescribed and the actual complex frequency transfer function. The prescribed transfer function would be defined in a wide frequency range and hence many analyses would be required for the accurate modeling – even with the use of Pade expansions. To the authors' knowledge nobody has yet solved such inverse problems in the frequency domain.

In the time domain it is relatively straightforward to design pulse modulation devices. The goal of the optimization is to minimize the least square energy norm of a prescribed target pulse shape and the actual pulse shape for a given input pulse shape. This objective function can be written as

$$\Phi = \int_0^T (U - U^*)^2 \, dt \,, \tag{41}$$

where $U = \sum_{t' \in N_t} u(t')^2 / N_t$ is the time averaged energy over one carrier wave-length, u is the electromagnetic field component (H_z or E_z) and N_t is a time window corresponding to the period of the carrier wavelength. Hence, if the objective function is 0 it means that the pulse envelope matches perfectly with the prescribed envelope function U^*. A 1D example of conversion of a Gaussian pulse to a longer rectangular pulse is shown in Fig. 7 (taken from [71]).

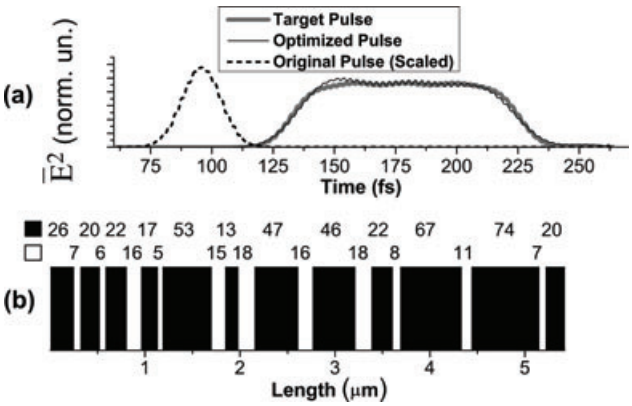

Figure 7 Design of 1D pulse shaping structure. Top: Input, target and optimized pulse shapes and bottom: 1D dielectric grating with dimensions resulting in above pulse response. From [71].

3.5. Plasmonics

Considering the other applications and developments above it is relatively easy to extend the topology optimization concept to photonic components that include metallic inclusions such as e. g. surface plasmonic devices. One of the material components in the material interpolation scheme (Eqs. (21) and (22)) is substituted with the permittivity (complex and often with a negative real part) of the metallic material.

As an example we consider the design of a grating coupler c. f. Fig. 8. A shape optimization of this device [72] resulted in a 50% transmission efficiency. A recent study [48] using the topology optimization approach resulted in an efficiency of 68% which, however, only can be obtained in practise if it is technologically possible to produce slanted groves. Imposing a vertical grove constraint on the problem resulted in a performance similar to the shape optimized design [72] proving that the real strength of topology optimization results depends on the amount of design freedom.

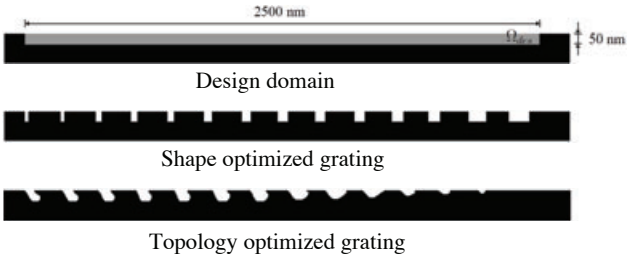

Figure 8 Design of surface grating coupler from [48]. Top: design domain indicated with grey, center: reference design from [72] with 50% coupling efficiency and bottom: topology optimized grating with 68% efficiency.

The topology optimization approach may rather straightforwardly be extended to three phase design by introducing another design variable for each element or grid point. The permittivity interpolation then becomes

$$\varepsilon_r = 1 + \rho((1-\rho_2)\varepsilon_{rd} + \rho_2\varepsilon_{rc} - 1) \tag{42}$$

where ε_{rc} and ε_{rd} are the relative permittivities of the conductor and dielectric, respectively. For this scheme design variable ρ determines the non-presence or presence of material and the second design variable ρ_2 determines the kind of material (dielectric or conductor). This idea has previously been used for e. g. negative thermal expansion material design [16] and multimaterial MEMS design [73] as well as for protein sequence design [74] and has also been applied to the design of nonlinear photonic devices as will be shown in the following section.

3.6. Non-linearities

Recently, there has been an increased focus on exploring nonlinear optical effects in order to create devices with improved or novel functionality [75–77]. This comprises bistable switches, diodes and limiters. The functionality of these devices relies on the Kerr effect that causes the permittivity ε_r to be a function of the electric field intensity.

In the frequency domain we can include this nonlinear effect in the analysis by considering a nonlinear Helmholtz equation [78]:

$$\nabla \cdot (A(u)\nabla u) + B(u)\omega^2 u = 0 \tag{43}$$

in which the two coefficients A and B can now be functions of the unknown field.

A number of interesting design problems can be formulated when nonlinear materials are available. In some cases functionalities can be obtained which are not possible with linear materials. In [78] the distribution of a linear and a nonlinear dielectric material was optimized in a 1D waveguide, that allowed for a different transmission of waves in the two directions – a diode structure which is not possible in the linear case. A three-material optimization problem was considered as well: air, a linear and a nonlinear dielectric material was distributed in a two-dimensional waveguide structure. The aim of the optimization problem was here to maximize the effect of the nonlinear material so that the transmission of the waves were reduced as much as possible when the input intensity increases – an optical limiter [79].

The optimization procedure is performed by solving two separate FE problems:

$$\mathbf{g}(\mathbf{u}_1, \gamma) - \mathbf{f} = \mathbf{0}, \tag{44}$$

$$\mathbf{S}\mathbf{u}_2 = \mathbf{f} \tag{45}$$

in which γ is the nonlinear parameter that quantifies the dependence of the permittivity on the intensity of the electric field. The first FE problem is nonlinear where the vector $\mathbf{g}$ represents the internal response that replaces the product $\mathbf{S}\mathbf{u}$ in the linear equation. This nonlinear equation can e. g. be solved by using an incremental Newton-Raphson algorithm [78]. The second equation is the corresponding linear FE problem which can be recovered from the nonlinear equation by setting $\gamma = 0$. By minimizing the following objective function

$$\Phi = c(\mathbf{u}_1) - c(\mathbf{u}_2) \tag{46}$$

in which $c(\mathbf{u}_1)$ measures the nonlinear response (e. g. the power flow though the waveguide) and $c(\mathbf{u}_2)$ the linear response, then we then create the largest possible reduction in the nonlinear transmission when compared to the linear transmission.

The optimized structure is shown in Fig. 9 where the linear and nonlinear responses are shown as well. The nonlinear response shows that the optimized material distribution modifies the transmission properties considerably when the input intensity increases. The proportionality between input and output intensity which is seen for a linear structure is gone and the transmission drops significantly for higher input intensities. The strong sensitivity to the input intensity is facilitated by a resonance mechanism where the large

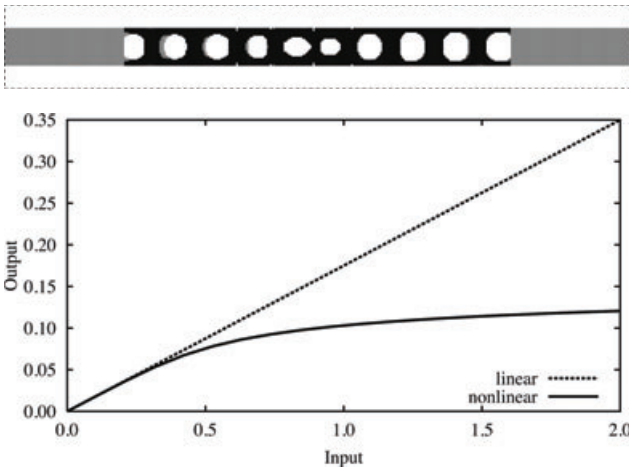

Figure 9 Top: optimal distribution of air (white), linear dielectric (grey) and nonlinear dielectric (black) in a two-dimensional waveguide structure. The objective is to maximize the nonlinear effect so that transmission of waves is reduced as much as possible when the input intensity increases. From [78].

linear transmission is obtained due to a tuned resonance in the structure. For larger input intensities the resonance in the nonlinear structure is shifted due to the intensity dependent refractive index. This leads to a significant drop in transmission.

3.7. Other related applications and methods

Apart from the already listed applications of the topology optimization method to nano-photonics there exist a number of applications and related methods that deserve mentioning.

Concerning applications, topology design of dispersion compensating optical fibers has been suggested in [80] and minimization of loss mechanisms for crystal fibres was suggested in [81]. Interesting applications that include coupled problems are still sparse but one example is optoelastic coupling as treated in [82, 83].

An open area of applications is within meta-material design. However, this area has a number of obstacles that make systematic optimization difficult. It is well-known that the extraction of effective properties for meta-materials has ambiguities in the selection of branches and hence if the physical properties are not uniquely determined it becomes impossible to optimize them. Furthermore, a number of papers have lately put question marks on the relevance on assigning effective material parameters to structures that a) have periodicities only slightly smaller than the wavelength and b) change material properties with the incident angle. For well-defined incident angle and single cell depth an initial topology optimization study for microwave meta-material design has been presented in [84].

A alternative approach to material distribution is the level-set approach [85]. This concept constitutes an alternative to the element based design description of topology optimization. For the level set approach the boundaries of the design are given as zero-level contour and design updates are based on boundary sensitivity analysis and updates using Hamilton-Jacobi based update formulations. This concept was first applied to topology optimization problems in mechanics [86, 87] and has since then in different forms been applied to problems in nano-photonics [57, 88–91].

Recently an inverse design procedure for nano-photonic structures using complementary convex optimization has been proposed [92]. The method is very similar to the topology optimization method but does in its present form not include penalization of intermediate densities and regularization techniques as discussed in 2.2 and 2.5 of this review.

4. Conclusions and outlook

Through a range of applications we have demonstrated the potential of the topology optimization method as an efficient tool for the design of nano-photonic systems.

The applications span photonic crystals with maximized bandgaps, photonic crystal waveguides and fibers with tailored propagation characteristics such as slow light or dispersion compensation and low-loss and broadband waveguide bend and splitters. Furthermore, we have demonstrated applications such as the design of pulseshaping structures, surface plasmon gratings and nonlinear photonic waveguides.

The general trend is that large improvements in performance can be obtained when we are allowed to find the optimal distribution of materials, free from geometrical constraints such as fixed square, circular or elliptical hole shape, or a regular hole placement. Modern fabrication techniques, combined with newly developed numerical techniques that allow control of the level of fine details in the optimized structures and ensure tolerance of the optimized design towards fabrication uncertainties, facilitate the transfer of optimized computed structures to real and highly efficient nano-photonic devices.

The range of problems that can benefit from topology optimization is in practise unlimited. In existing fields new specific optimization problems emerge constantly. Industrial applications in mechanics-based topology optimization has reached a high level of maturity and the method is often used in the conceptual design phase followed by more detailed shape and size optimization studies. A similar tendency can be expected in the field of nano-photonic device design. Future applications can be expected to involve a complicated interplay of physical disciplines, such as already seen in opto-mechanical actuators and opto-fluidic systems as well as quantum-dot based photonic devices. Considering the complex physical phenomena involved in coupled processes combined with the lack of the necessary intuition and analytical solutions, it is believed that the design process of such systems can benefit immensely from numerical material distribution design tools such as topology optimization.

Acknowledgements. This work was supported by grants from the Danish Center of Scientific Computing (DCSC) and by a Eurohorcs/ESF European Young Investigator Award (EURYI, http://www.esf.org/euryi) through the grant “Synthesis and topology optimization of optomechanical systems”. Useful discussions and collaborations with members of the TopOpt-group (www.topopt.dtu.dk) and Department of Photonics Engineering, DTU are gratefully acknowledged.

Received: 29 June 2010, **Revised:** 25 October 2010,
Accepted: 22 November 2010

Published online: 16 December 2010

Key words: Topology optimization, nano-photonics, material distribution, sensitivity analysis, math-programming.

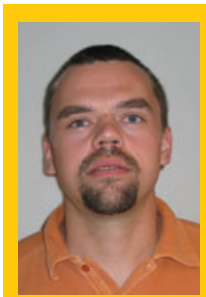

Jakob S. Jensen is an Associate Professor at the Department of Mechanical Engineering, Technical University of Denmark (DTU). He obtained his Ph. D. degree in 1999 and acquired 2½ years of industrial experience before pursuing his research carrier in academia. Research interests include linear and nonlinear dynamics of mechanical systems and topology optimization of vibration and wave propagation problems.

Ole Sigmund is a Professor at the Department of Mechanical Engineering, Technical University of Denmark (DTU). He obtained his Ph. D. degree 1994 and Habilitation in 2001 and has had research positions at University of Essen and Princeton University. He is a member of the Danish Academy of Technical Sciences and the Royal Academy of Science and Letters (Denmark) and is the chairman of the Danish Center for Applied Mathematics and Mechanics (DCAMM). Research interests include theoretical extensions and applications of topology optimization methods to mechanics and multiphysics problems.

References

[1] E. Yablonovitch, Phys. Rev. Lett. **58**(20), 2059–2062 (1987).
[2] S. John, Phys. Rev. Lett. **58**(23), 2486–2489 (1987).
[3] T. F. Krauss, R. M. D. L. Rue, and S. Brand, Nature **383**, 699–702 (1996).
[4] W. L. Barnes, A. Dereux, and T. W. Ebbesen, Nature **424**(6950), 824830 (2003).
[5] J. Pendry, Phys. Rev. Lett. **85**, 3966 (2000).
[6] T. Ebbesen, H. Lezec, H. Ghaemi, T. Thio, and P. Wolff, Nature **391**(6668), 667–669 (1998).
[7] J. B. Pendry, D. Schurig, and D. R. Smith, Science **312**(5781), 1780–1782 (2006).
[8] U. Leonhardt, Science **312**(5781), 1777–1780 (2006).
[9] J. D. Joannopoulos, R. D. Meade, and J. N. Winn, Photonic Crystals: Molding the Flow of Light (Princeton University Press, Princeton, Oxford, 1995).
[10] L. Sanchis, A. Hakansson, D. Lopez-Zanon, J. Bravo-Abad, and J. Sanchez-Dehesa, Appl. Phys. Lett. **84**(22), 4460–4462 (2004).
[11] A. Kildishev, U. Chettiar, Z. Liu, V. Shalaev, D. H. Kwon, Z. Bayraktar, and D. H. Werner, J. Opt. Soc. Am. B **24**, A34–A39 (2007).
[12] O. Sigmund and K. Hougaard, Phys. Rev. Lett. **100**(15), 153904 (2008).
[13] M. P. Bendsøe and N. Kikuchi, Comput. Methods Appl. Mech. Eng. **71**(2), 197–224 (1988).
[14] M. P. Bendsøe and O. Sigmund, Topology Optimization – Theory, Methods and Applications (Springer Verlag, Berlin, Heidelberg, 2003).
[15] U. D. Larsen, O. Sigmund, and S. Bouwstra, IEEE J. Microelectromech. Syst. **6**(2), 99–106 (1997).
[16] O. Sigmund and S. Torquato, Appl. Phys. Lett. **69**(21), 3203–3205 (1996).
[17] O. Sigmund, Comput. Methods Appl. Mech. Eng. **190**(49–50), 6577–6604 (2001).
[18] T. Borrvall and J. Petersson, Int. J. Num. Methods Fluids **41**, 77–107 (2003).
[19] O. Sigmund and J. S. Jensen, Philos. Trans. R. Soc. A, Math. Phys. Eng. Sci. **361**, 1001–1019 (2003).
[20] G. Kiziltas, D. Psychoudakis, J. L. Volakis, and N. Kikuchi, IEEE Trans. Antennas Propag. **51**, 2732–2743 (2003).
[21] A. Erentok and O. Sigmund, IEEE Trans. Antennas Propag., online (2010).
[22] M. Burger, S. Osher, and E. Yablonovitch, IEICE Trans. Electron. **E87-C**(3), 258–265 (2004).
[23] M. Dühring, J. S. Jensen, and O. Sigmund, J. Sound Vibr. **317**, 557–575 (2008).
[24] J. P. Berenger, J. Comput. Phys. **114**(2), 185–200 (1994).
[25] M. Koshiba, Y. Tsuji, and S. Sasaki, IEEE Microw. Wirel. Compon. Lett. **11**(April), 152–154 (2001).
[26] R. Matzen, J. S. Jensen, and O. Sigmund, J. Opt. Soc. Am. B, Opt. Phys. **27**(10), 2040–2050 (2010).
[27] W. Axmann and P. Kuchment, J. Comput. Phys. **150**(2), 468–481 (1999).
[28] J. S. Jensen and O. Sigmund, J. Opt. Soc. Am. B, Opt. Phys. **22**(6), 1191–1198 (2005).
[29] M. P. Bendsøe, Struct. Optim. **1**, 193–202 (1989).
[30] M. P. Bendsøe and O. Sigmund, Arch. Appl. Mech. **69**(9–10), 635–654 (1999).
[31] Y. Tsuji, K. Hirayama, T. Nomura, K. Sato, and S. Nishiwaki, IEEE Photon. Technol. Lett. **18**(5–8), 850–852 (2006).
[32] J. C. Bellido and A. Donoso, J. Optim. Theory Appl. **134**(2), 339–352 (2007).
[33] A. P. Seyranian, E. Lund, and N. Olhoff, Struct. Optim. **8**(4), 207–227 (1994).
[34] N. L. Pedersen, Struct. Multidisc. Optim. **20**, 2–11 (2000).
[35] D. A. Tortorelli and P. Michaleris, Inv. Probl. Eng. **1**, 71–105 (1994).
[36] K. Svanberg, Int. J. Num. Methods Eng. **24**, 359–373 (1987).
[37] O. Sigmund and J. Petersson, Struct. Optim. **16**(1), 68–75 (1998).
[38] O. Sigmund, Struct. Multidisc. Optim. **33**(4–5), 401–424 (2007).
[39] O. Sigmund, Mech. Struct. Mach. **25**(4), 493–524 (1997).
[40] T. E. Bruns and D. A. Tortorelli, Comput. Methods Appl. Mech. Eng. **190**(26–27), 3443–3459 (2001).
[41] B. Bourdin, Int. J. Num. Methods Eng. **50**(9), 2143–2158 (2001).
[42] J. Guest, J. Prevost, and T. Belytschko, Int. J. Num. Methods Eng. **61**(2), 238–254 (2004).
[43] J. Guest, Comput. Methods Appl. Mech. Eng. **199**(1–4), 123–135 (2009).
[44] O. Sigmund, Acta Mech. Sin. **25**(2), 227–239 (2009).
[45] F. Wang, J. S. Jensen, and O. Sigmund, J. Opt. Soc. Am. B, Opt. Phys. submitted (2010).
[46] F. Wang, B. Lazarov, and O. Sigmund, Struct. Multidisc. Optim. (2010), DOI 10.1007/s00158-010-0602-y.
[47] R. Stainko and O. Sigmund, Waves Random Complex Media **17**, 477–489 (2007).
[48] J. Andkjær, S. Nishiwaki, T. Nomura, and O. Sigmund, JOSA B **27**(9), 1828–1832 (2010).
[49] S. J. Cox and D. C. Dobson, SIAM J. Appl. Math. **59**(6), 2108–2120 (1999).
[50] S. J. Cox and D. C. Dobson, J. Comput. Phys. **158**(2), 214–224 (2000).
[51] M. Rechtsman, H. C. Jeong, P. Chaikin, S. Torquato, and P. Steinhardt, Phys. Rev. Lett. **101**(7) (2008).
[52] T. Nomura, S. Nishiwaki, K. Sato, and K. Hirayama, Fin. Elem. Anal. Des. **45**(3), 210–226 (2009).
[53] L. H. Frandsen, A. V. Lavrinenko, J. Fage-Pedersen, and P. I. Borel, Opt. Express **14**(20), 9444–9450 (2006).
[54] M. Settle, R. Engelen, M. Salib, A. Michaeli, L. Kuipers, and T. Krauss, Opt. Express **15**(1), 219–226 (2007).

[55] J. S. Jensen and O. Sigmund, Appl. Phys. Lett. **84**(12), 2022–2024 (2004).
[56] A. Mekis, J. C. Chen, I. Kurland, S. Fan, P. R. Villeneuve, and J. D. Joannopoulos, Phys. Rev. Lett. **77**(18), 3787–3790 (1996).
[57] W. R. Frei, D. A. Tortorelli, and H. T. Johnson, Appl. Phys. Lett. **86**(11), 111114 (2005).
[58] P. I. Borel, A. Harpøth, L. H. Frandsen, M. Kristensen, J. S. Jensen, P. Shi, and O. Sigmund, Opt. Express **12**(9), 1996–2001 (2004).
[59] T. Uusitupa, K. Karkkainen, and K. Nikoskinen, Microw. Opt. Technol. Lett. **39**(4), 326–333 (2003).
[60] L. H. Frandsen, A. Harpøth, P. I. Borel, M. Kristensen, J. S. Jensen, and O. Sigmund, Opt. Express **12**(24), 5915–5921 (2004).
[61] P. I. Borel, L. H. Frandsen, A. Harpøth, M. Kristensen, J. S. Jensen, and O. Sigmund, Electron. Lett. **41**(2), 69–71 (2005).
[62] J. S. Jensen, O. Sigmund, L. H. Frandsen, P. I. Borel, A. Harpøth, and M. Kristensen, IEEE Photon. Technol. Lett. **41**(2), 69–71 (2005).
[63] N. Ikeda, Y. Sugimoto, Y. Watanabe, N. Ozaki, A. Mizutani, Y. Takata, J. S. Jensen, O. Sigmund, P. Borel, M. Kristensen, and K. Asakawa, Electron. Lett. **42**(18), 1031–1033 (2006).
[64] L. Yang, A. V. Lavrinenko, L. H. Frandsen, P. I. Borel, A. Tetu, and J. Fage-Pedersen, Electron. Lett. **43**(17), 923–924 (2007).
[65] P. I. Borel, B. B. Olsen, L. H. Frandsen, T. Nielsen, J. Fage-Pedersen, A. Lavrinenko, J. S. Jensen, O. Sigmund, and A. Kristensen, Opt. Express **15**(3), 1261–1266 (2007).
[66] J. S. Jensen and O. Sigmund, Topology optimization of wave-propagation problems, in: IUTAM Symposium on Topological Design Optimization of Structures, Machines and Materials: Status and Perspectives, , Solid Mechanics and its Applications; 137 (Springer, Dordrecht, The Netherlands, 2006), pp. 387–390.
[67] Y. Tsuji and K. Hirayama, IEEE Photon. Technol. Lett. **20**(9–12), 982–984 (2008).
[68] S. Nishiwaki, T. Nomura, S. Kinoshita, K. Izui, M. Yoshimura, K. Sato, and K. Hirayama, Finite Elem. Anal. Des. **45**(12), 944–957 (2009).
[69] J. S. Jensen and O. Sigmund, Phononic bandgap structures as optimal designs, in: IUTAM Symposium on Asymptotics, Singularities and Homogenization in Problems of Mechanics, Liverpool, UK, 8–11 July, 2002, edited by A. B. Movchan (Kluwer Academic Publishers, 2003), pp. 71–81.
[70] J. Dahl, J. S. Jensen, and O. Sigmund, Struct. Multidisc. Optim. **36**, 585–595 (2008).
[71] L. Yang, A. V. Lavrinenko, J. M. Hvam, and O. Sigmund, Appl. Phys. Lett. **95**, 261101 (2009).
[72] J. Lu, C. Petre, E. Yablonovitch, and J. Conway, J. Opt. Soc. Am. **24**(9), 2268–2272 (2007).
[73] O. Sigmund, Comput. Methods Appl. Mech. Eng. **190**(49–50), 6605–6627 (2001).
[74] S. Koh, G. Ananthasuresh, and S. Vishveshwara, Int. J. Robotics Design **24**(2–3), 109–130 (2005).
[75] C. Koos, L. Jacome, C. Poulton, J. Leuthold, and W. Freude, Opt. Express **15**(10), 5976–5990 (2007).
[76] J. Bravo-Abad, S. Fan, S. G. Johnson, J. D. Joannopoulos, and M. Soljačić, J. Lightwave Technol. **25**(9), 2539–2546 (2007).
[77] M. A. Foster, A. C. Turner, M. Lipson, and A. L. Gaeta, Opt. Express **16**(2), 1300–1320 (2008).
[78] J. S. Jensen, Struct. Multidisc. Optim. submitted (2010).
[79] M. Scalora, J. P. Dowling, C. M. Bowden, and M. J. Bloemer, Phys. Rev. Lett. **73**, 1368–1371 (1994).
[80] J. Riishede and O. Sigmund, J. Opt. Soc. Am. B, Opt. Phys. **25**(1), 88–97 (2008).
[81] M. B. Dühring, O. Sigmund, and T. Feurer, J. Opt. Soc. Am. B, Opt. Phys. **27**, 51–58 (2010).
[82] M. B. Dühring and O. Sigmund, J. Appl. Phys. **105**, 083529 (2009).
[83] A. Gersborg and O. Sigmund, Int. J. Num. Methods Eng., to appear (2010).
[84] A. Diaz and O. Sigmund, Struct. Multidisc. Optim. **41**(2), 163–177 (2010).
[85] S. Osher and J. Sethian, J. Comput. Phys. **79**(1), 12–49 (1988).
[86] M. Wang, X. Wang, and D. Guo, Comput. Methods Appl. Mech. Eng. **192**(1–2), 227–246 (2003).
[87] G. Allaire, F. Jouve, and A. M. Toader, J. Comput. Phys. **194**(1), 363–393 (2004).
[88] C. Kao, S. Osher, and E. Yablonovitch, Appl. Phys. B (Lasers Opt.) **B81**(2–3), 235–244 (2005).
[89] W. Frei, H. Johnson, and K. Choquette, J. Appl. Phys. **103**(3) (2008).
[90] W. Frei, D. Tortorelli, and H. Johnson, Opt. Letters **32**(1), 77–79 (2007).
[91] W. Frei, H. Johnson, and D. Tortorelli, Comput. Methods Appl. Mech. Eng. **197**(41–42), 3410–3416 (2008).
[92] J. Lu and J. Vučkovič, Opt. Express **18**(4), 3793 (2010).